# Structure of Dipalmitoylphosphatidylcholine/Cholesterol Bilayer at Low and High Cholesterol Concentrations: Molecular Dynamics Simulation

Alexander M. Smondyrev and Max L. Berkowitz
Department of Chemistry, University of North Carolina at Chapel Hill, Chapel Hill, North Carolina 27599 USA

ABSTRACT By using molecular dynamics simulation technique we studied the changes occurring in membranes constructed of dipalmitoylphosphatidylcholine (DPPC) and cholesterol at 8:1 and 1:1 ratios. We tested two different initial arrangements of cholesterol molecules for a 1:1 ratio. The main difference between two initial structures is the average number of nearest-neighbor DPPC molecules around the cholesterol molecule. Our simulations were performed at constant temperature ($T$ = 50°C) and pressure ($P$ = 0 atm). Durations of the runs were 2 ns. The structure of the DPPC/cholesterol membrane was characterized by calculating the order parameter profiles for the hydrocarbon chains, atom distributions, average number of *gauche* defects, and membrane dipole potentials. We found that adding cholesterol to membranes results in a condensing effect: the average area of membrane becomes smaller, hydrocarbon chains of DPPC have higher order, and the probability of *gauche* defects in DPPC tails is lower. Our results are in agreement with the data available from experiments.

## INTRODUCTION

It is now well-known that the presence of cholesterol is required for normal functioning of mammalian plasma membranes. To better understand how cholesterol influences the properties of natural membranes one studies the effect of cholesterol on phospholipid membranes first. While a large amount of research was done to investigate the effect of cholesterol on physical properties of phospholipid membranes, molecular-level understanding of changes in these properties is still incomplete (McMullen and McElhaney, 1996). It is known that the addition of cholesterol to phospholipid membranes produces a reach phase diagram of the mixture. Such a phase diagram was recently mapped out for dipalmitoylphosphatidylcholine (DPPC)/cholesterol in the presence of water (Vist and Davis, 1990). It was shown that when a substantial amount of cholesterol is added to DPPC membrane, a new phase is formed that has properties of a liquid and a solid. According to the classification introduced by Zuckermann et al. (1993) the new phase that appears in the cholesterol/phospholipid mixture is called a liquid-ordered phase, while the gel phase is called a solid-ordered phase and the liquid crystal phase is called a liquid-disordered phase. In this classification the liquid or solid description refers to the order in the translational degrees of freedom, while the ordered or disordered description is reserved for the conformational degrees of freedom. At small amounts of cholesterol one observes the usual two phases: solid-ordered and liquid-disordered. The transition from the solid-ordered to liquid-disordered phase occurs at ~40°C. When the amount of cholesterol in DPPC is rather large (>25 mol %) the liquid-ordered phase is present. Interestingly enough, no phase transition to solid-ordered phase is observed with lowering the temperature. To gain more understanding of the properties of phospholipid membranes in the presence of cholesterol on a molecular level, one can perform detailed computer simulations. Recently, three such simulations were described in the literature. Two of the simulations dealt with a dimyristoylphosphatidylcholine (DMPC)/cholesterol mixture (Robinson et al., 1995; Gabdouline et al., 1996), and one with a DPPC/cholesterol mixture (Tu et al., 1998). In the simulations of Robinson et al. and Tu et al. the study was done at low content of cholesterol, while the simulation of Gabdoulline et al. was performed at high content of cholesterol (50 mol %). The simulation of Robinson et al. was performed under constant volume conditions, so that effects of cholesterol on geometrical properties of membrane could not be investigated. They characterized the effect of cholesterols on membrane structure and dynamics in great detail, but their time scale (400 ps) may not be sufficiently long for convergence. Gabdouline et al. studied the properties of DMPC membrane with 50 mol % cholesterol at different temperatures. The last 100 ps of their simulation was used for data analysis, which is too short to accurately sample the motions of cholesterol molecules and conformations of lipid hydrocarbon tails. The results of their pure DMPC control simulation should be regarded with caution, since the area per lipid was much smaller than the experimental value. To understand the systematic changes in the phospholipid membrane on a nanosecond time scale when a small amount of cholesterol is added to it and when a large amount of cholesterol is present in the membrane, we performed 2-ns simulations on a DPPC/cholesterol bilayer when the amount of cholesterol was 11 and 50 mol %. The data from these simulations were compared to the data from our previous simulations on pure DPPC membrane (Smondyrev and Berkowitz, 1999a).

*Received for publication 8 March 1999 and in final form 2 July 1999.*
Address reprint requests to Dr. Max Berkowitz, Dept. of Chemistry CB3290, University of North Carolina, Chapel Hill, NC 27599-3290. Tel.: 919-962-1218; Fax: 919-962-2388; E-mail: max@unc.edu.

0006-3495/99/10/2075/15 $2.00

## METHODS

We used the same united atom force field for DPPC molecules that we employed in our recent simulations of DPPC/water (Smondyrev and Berkowitz, 1999a,b) and DPPC/dimethylsulfoxide (DMSO) systems (Smondyrev and Berkowitz, 1999c). Parameters for the cholesterol molecules were taken from the united atom AMBER force field (Weiner et al., 1984) and partial atomic charges were calculated using the Gaussian 98 program at the 6-31G(d) basis set level and the Mulliken population analysis (Frisch et al., 1998). The structures of the cholesterol molecules with atomic labels are shown in Fig. 1, and partial atomic charges are given in Table 1. The water model employed in our simulations was TIP3P (Jorgensen et al., 1983).

We performed three simulations of the DPPC/cholesterol system. In one, the simulation membrane contained a low amount of cholesterol (11 mol %), and in two others the cholesterol level in the bilayer was high (50 mol %). In simulations with high levels of cholesterol the distributions of sterol molecules in the membrane differed, as we shall explain below. The initial configuration was prepared in several steps. First, we created a monolayer containing DPPC and cholesterol molecules. Coordinates of DPPC molecules were obtained by adding two carbon atoms to each tail of the DMPC molecule coordinates determined by Vanderkooi (1991). Coordinates of cholesterol molecules were taken from the crystal structure (Shieh et al., 1981). To create a monolayer for a system with DPPC/cholesterol at an 8:1 ratio (11 mol % cholesterol) we placed 36 lipid molecules on the sites of the hexagonal lattice. Then four DPPC molecules were replaced with cholesterol molecules, so that the distance between cholesterol molecules was at its maximum. This distribution of cholesterol molecules in lipid bilayer was similar to the one used in a recent simulation of a DMPC/cholesterol system (Robinson et al., 1995). In this arrangement each cholesterol molecule is completely solvated by the lipid's hydrocarbon chains.

Molecular packing of DMPC and cholesterol in structures A and B reported by Vanderkooi (1994) was used to construct the monolayers of DPPC/cholesterol at ratios 1:1. Each monolayer contained 32 molecules: 16 of DPPC and 16 of cholesterol. The difference between structures A and B can be seen in Fig. 2. In structure A, cholesterol molecules alternate with DPPC molecules, so that nearest-neighbor interactions occur between DPPC and cholesterol molecules. In structure B, strips of cholesterol molecules are placed between strips of DPPC molecules, so that interactions between like molecules (DPPC:DPPC or cholesterol:cholesterol) are predominant. It should be pointed out that our choice of initial arrangement is not unique. Recent experiments provided evidence for the regular distribution of cholesterol molecules with sterol molecules maximally separated (Chong, 1994). This arrangement is similar to structure A used in our work. Other possibilities include random distributions of cholesterol molecules, coexisting cholesterol-rich and -poor domains, and regular arrays of sterol molecules (for review see McMullen and McElhaney, 1996). Computer simulations allow us to perform comparative studies of membranes with predetermined arrangements of cholesterol molecules. By studying two very distinct DPPC/cholesterol bilayers (structures A and B) we attempt to provide information on changes of structural properties of sterol-containing membranes as a function of cholesterol distribution. After constructing the initial structures, the preparation method described below was the same for all three systems. Each monolayer was equilibrated for 20 ps with phosphorus atoms of DPPC and all cholesterol atoms held fixed. After this step, the final configuration of the monolayer was used to construct the bilayer using the appropriate symmetry group (Vanderkooi, 1994). The bilayer was equilibrated for another 20 ps with the same constraints. Water molecules were then added to the bilayer, so that the number of water molecules per molecule in the membrane was $n_W = 20.5$, as in our previous simulations of pure DPPC bilayer (Smondyrev and Berkowitz, 1999a). The total number of water molecules in the simulation of DPPC + 11 mol % cholesterol was 1476. Bilayers with 50 mol % cholesterol were surrounded by 1312 water molecules. The interlamellar spacing was then gradually decreased, allowing the system to equilibrate for 2 ps at each step. After adjusting the dimensions of the simulation cells we performed a 50-ps simulation with free phosphorus atoms allowing DPPC molecules to move freely. Cholesterol rings were held fixed, but the cholesterol tail and hydroxyl group were not constrained. Keeping atoms in cholesterol rings frozen, we increased the temperature to 423 K and then reduced it in a series of 20-ps simulations ($T$ = 393, 363, 343, 333, and 323 K) to ensure that DPPC and cholesterol tails are disordered. Finally, all atoms were allowed to move and the system was equilibrated at $T$ = 323 K for another 100 ps.

After equilibrating the system at constant volume we performed a simulation at constant pressure ($P$ = 0 atm) and temperature ($T$ = 323 K) with periodic boundary conditions. We kept angles of the simulation cell fixed and varied the dimensions of the cell using a Hoover barostat. Thermostat and barostat relaxation times were, correspondingly, 0.2 ps and 0.5 ps. All bond lengths were constrained using the SHAKE algorithm with a tolerance of $10^{-4}$, allowing us to use the time step of 0.002 ps. The Ewald summation technique was employed to calculate electrostatic contributions with a tolerance of $10^{-4}$. The real-space part of the Ewald sum and van der Waals interactions were cut off at 10 Å. The length of each constant-pressure run was 2 ns. Calculations were performed on Cray-T3E at the San Diego Supercomputer Center and Texas Advanced Computing Center using the DL_POLY simulation package version 2.8 developed in the Daresbury Laboratory, N. Warrington, England (Smith and Forester, 1996).

**TABLE 1 Partial atomic charges for cholesterol molecules**

| Atom | Charge | Atom | Charge | Atom | Charge |
|---|---|---|---|---|---|
| C1 | 0.012 | C11 | 0.015 | C21 | 0 |
| C2 | −0.013 | C12 | 0.024 | C22 | 0.017 |
| C3 | 0.347 | C13 | −0.080 | C23 | −0.004 |
| C4 | 0.046 | C14 | −0.002 | C24 | 0.013 |
| C5 | −0.007 | C15 | 0.010 | C25 | −0.028 |
| C6 | −0.051 | C16 | −0.001 | C26 | 0.007 |
| C7 | 0.029 | C17 | 0.015 | C27 | 0.007 |
| C8 | −0.001 | C18 | 0.026 | O | −0.694 |
| C9 | 0.003 | C19 | 0.046 | H | 0.343 |
| C10 | −0.070 | C20 | −0.009 | | |

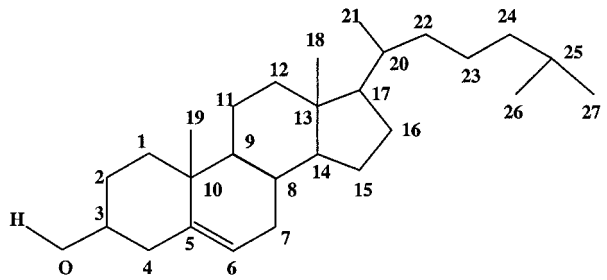


FIGURE 1 Structure of cholesterol molecule. Carbon atoms are labeled with numbers, hydrogens are not shown except for the one in the hydroxyl group.

## RESULTS

Let us first examine the changes in the bilayer geometry due to the inclusion of cholesterol. In Fig. 3 we show the area of the heterodimer of DPPC and cholesterol in simulations with 50 mol % cholesterol as a function of time. After ~1000 ps, areas in both simulations mostly converged to their corresponding plateau values. For structure A, the area per heterodimer continued to drift slowly even after the first 1 ns of simulation. The average change in its value during

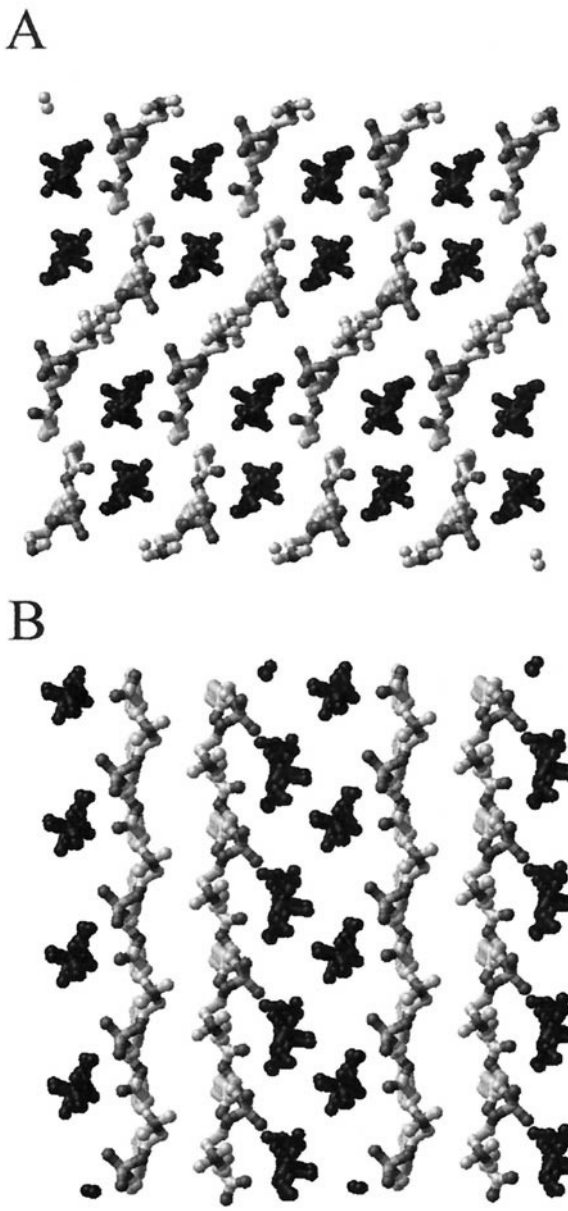


FIGURE 2 Initial structures of membrane with 50 mol % cholesterol. DPPC molecules are shown in gray, cholesterols in black.

the last 1 ns was $\sim$1 Å$^2$. This may indicate that when sterol is distributed uniformly in membrane, the system is trapped in a metastable state. Using the data for the last 1 ns we determined the average values of the heterodimer areas: 78.5 $\pm$ 0.8 Å$^2$ and 76.7 $\pm$ 0.6 Å$^2$ for structures A and B, respectively. We should mention here that determining the value for the area per dimer is a suitable method to describe the geometries of systems with equal amounts of lipid and cholesterol, but we cannot use it for systems with, for example, low cholesterol content. Moreover, we would like to know the average area occupied by a DPPC molecule in the presence of cholesterol in order to compare it with the value found in the simulations of pure DPPC bilayers. To extract the area per DPPC molecule we need to know the

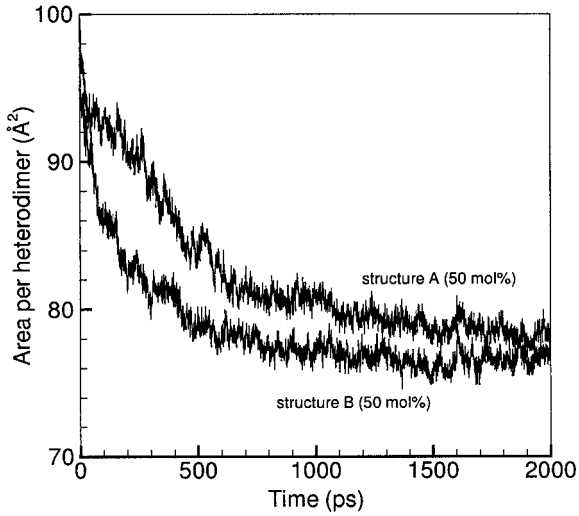


FIGURE 3 Area per DPPC:cholesterol heterodimer for structures A (*top curve*) and B (*lower curve*) in bilayers with 50 mol % cholesterol.

area of a cholesterol molecule. This value was determined by different authors and varied in the range from 26 to 39 Å$^2$ (Craven and DeTitta, 1976; Pearson and Pascher, 1979; Hyslop et al., 1990; Almeida et al., 1992; Chong, 1994). For our estimates we adopted $A_{\text{chol}}$ = 32 Å$^2$ (Ipsen et al., 1990; Engelman and Rothman, 1972), which is similar to the area of the cholesterol molecule (32.4 Å$^2$) obtained in recent simulations of the DPPC/cholesterol bilayer (Tu et al., 1998). Therefore, to get an estimate for the area per DPPC molecule in the simulation with 11 mol % cholesterol, we subtracted from the total area per monolayer the total average area occupied by sterol molecules (4 $\times$ 32 Å$^2$) and divided the difference by the number of lipids in monolayer (32 molecules). The time evolution of the area per DPPC molecule obtained for a system with 11 mol % cholesterol

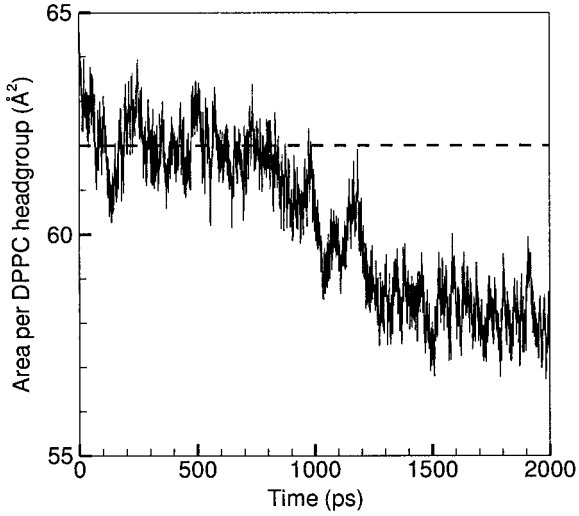


FIGURE 4 Area per DPPC molecule in bilayer with 11 mol % cholesterol. Horizontal dashed line shows the average area per lipid headgroup in pure DPPC membrane.

is shown in Fig. 4. During the first 800 ps of simulation the area per DPPC molecule remained close to the value in the pure DPPC bilayer. After ~1 ns it dropped to a lower value and remained stable for the remainder of our run. The average value of the area per DPPC molecule calculated during the last 750 ps of simulation was 58.3 ± 0.6 Å$^2$. If we use the same value for the area per cholesterol (32 Å$^2$) in cases when the simulations are done with 50 mol % sterol, the average areas per DPPC molecule would be 46.5 and 44.7 Å$^2$, respectively. The average values of the interlamellar spacing (see Table 2) increase accordingly. This is partially due to the thickening of the water layer due to the reduction in membrane area. In addition, the thickness of the membrane becomes larger and contributes to the total increase in repeat periods. Recent simulations of DPPC/cholesterol bilayer at 12.5 mol % cholesterol (Tu et al., 1998) did not reveal any change in the average area per DPPC molecule. Mean-field calculations and Monte Carlo simulations of DPPC/cholesterol bilayers (Zuckermann et al., 1993) indicate that the area per DPPC is decreasing with the increasing concentration of cholesterol. For 0, 10, and 45 mol % cholesterol the area per DPPC molecule was 64.5, 60, and 42 Å$^2$ from mean-field calculations and 64.7, 60.3, and 46.5 from model MC simulations. Our recent simulation of the pure DPPC bilayer (Smondyrev and Berkowitz, 1999a) gave an average area per DPPC headgroup of 61.6 Å$^2$. As we can see, the area per DPPC molecule decreases with the increase in cholesterol content similarly to the results of Zuckermann et al. (1993) and even at 11 mol % cholesterol changes by almost 4 Å$^2$.

In Fig. 5 we show the side view of lipid bilayer with 11 mol % cholesterol. Cholesterol molecules exhibit high translational and orientational freedom of motion. We can see that they can move toward the bilayer center and away from it. They can also tilt with respect to bilayer normal and rotate around the bilayer normal. Both DPPC and cholesterol hydrocarbon tails are in disordered state. In bilayers with 50 mol % cholesterol (Fig. 5) the structure of membrane is different. DPPC and sterol hydrocarbon tails are more ordered and cholesterol molecules are aligned more parallel to the bilayer normal. Although there is more translational order in membrane compared to a system with low cholesterol content, it is not as high as in bilayers in gel phase. This behavior is expected for lipid/cholesterol bilayers in the liquid-ordered phase. Cholesterol hydroxyl groups are located at approximately the same distance from the bilayer center as the DPPC ester groups. In Fig. 6 we show pictures of bilayer halves at 50 mol % cholesterol (structures A and B) when looking at the surface of the membrane, and at the tails of lipid and cholesterol molecules looking from the center of bilayer. Close to the bilayer center lipid's hydrocarbon tails and cholesterol molecules are densely packed. There is little free volume between them and we can clearly identify regions occupied by lipids and cholesterols. At the membrane surface the situation is very different. Cholesterol molecules are covered by DPPC headgroups and sometimes become obscured from view. The surface of the membrane is rough and there are voids between lipid molecules occupied by water (this is also evident when looking at the side views of membranes, Fig. 5) through which it can penetrate deeper inside the bilayer. It becomes evident now that results for the area per DPPC molecule should be interpreted more carefully. The values for the areas per DPPC molecule at different sterol concentrations obtained earlier, namely 58.3, 46.5, and 44.7 Å$^2$ at 11 and 50 mol % cholesterol, should be viewed as the area per DPPC hydrocarbon tails. Since cholesterol is buried in the tail region we can estimate the area available for the DPPC headgroups at 50 mol % as the area per DPPC/cholesterol heterodimer, which is ~77.6 Å$^2$ in structures A and B. This is almost 30% larger than the area per headgroup in pure DPPC membranes. As we can see from the present discussion, the area per DPPC molecule in the 1:1 DPPC:cholesterol mixture is a notion that is somewhat confusing. If measured as the area per headgroup, it is ~77.6 Å$^2$, while if measured as the area per tails, it is ~45.6 Å$^2$.

Despite the fact that the average area per DPPC headgroup is larger in membranes with 50 mol % cholesterol compared to pure DPPC bilayers, lipid headgroups have a higher probability to point toward the water layer in bilayers with cholesterol, rather than to orient parallel to the bilayer surface, as in pure DPPC bilayers. This is also evident from the distributions of the cosines of the angle between vector-connecting phosphorus and nitrogen atoms in the DPPC headgroup and bilayer normal (see Fig. 7). The average values of this angle are listed in Table 2. In pure DPPC bilayers the cosine distribution is almost uniform, indicating that P-N vectors have almost equal probabilities to point either toward the water layer or bilayer interior. The addition of 50 mol % cholesterol to lipid membrane reduces the probability of finding the P-N vector pointing toward the bilayer interior. Above some threshold value the distribution is almost uniform. In bilayers with 11 mol % cholesterol the distribution has features seen in pure membranes and membranes with 50 mol % cholesterol. There is a

**TABLE 2 Average values of the area per DPPC molecule, lamellar spacing, angle between P-N vector, and bilayer surface and distances from bilayer center to atoms in DPPC molecules**

| | 0 mol % | 11 mol % | 50 mol % (A) | 50 mol % (B) |
|---|---|---|---|---|
| Area DPPC | 61.6 ± 0.6 | 58.3 ± 0.6 | 46.5 ± 0.6 | 44.7 ± 0.6 |
| L | 59.0 ± 1.0 | 63.0 ± 0.6 | 76.0 ± 0.6 | 77.9 ± 0.6 |
| P-N tilt | 9 | 16 | 18.8 | 22.0 |
| P | 19.0 ± 2.0 | 20.0 ± 1.9 | 22.1 ± 1.2 | 23.2 ± 1.2 |
| $C_\gamma$ | 19.5 ± 3.6 | 21.1 ± 3.6 | 23.4 ± 2.4 | 24.4 ± 2.6 |
| $C_\alpha$ | 19.5 ± 2.5 | 20.8 ± 2.6 | 22.8 ± 2.0 | 24.0 ± 2.0 |
| $C_\beta$ | 19.4 ± 2.9 | 20.7 ± 3.0 | 22.7 ± 1.7 | 23.7 ± 1.8 |
| $C_{G3}$ | 17.2 ± 2.0 | 18.1 ± 1.9 | 20.2 ± 1.4 | 21.5 ± 1.2 |
| $C_4$ | 11.7 ± 1.9 | 12.6 ± 1.8 | 14.8 ± 1.3 | 15.5 ± 1.1 |
| $C_5$ | 10.8 ± 1.9 | 11.7 ± 1.8 | 13.6 ± 1.4 | 14.3 ± 1.2 |
| $C_9$ | 7.1 ± 1.9 | 7.8 ± 1.8 | 8.9 ± 1.4 | 9.5 ± 1.2 |
| $C_{14}$ | 3.2 ± 1.7 | 3.3 ± 2.0 | 3.2 ± 1.8 | 2.8 ± 1.1 |
| $C_{15}$ | 2.1 ± 2.4 | 2.3 ± 2.5 | 2.3 ± 2.2 | 1.9 ± 1.2 |

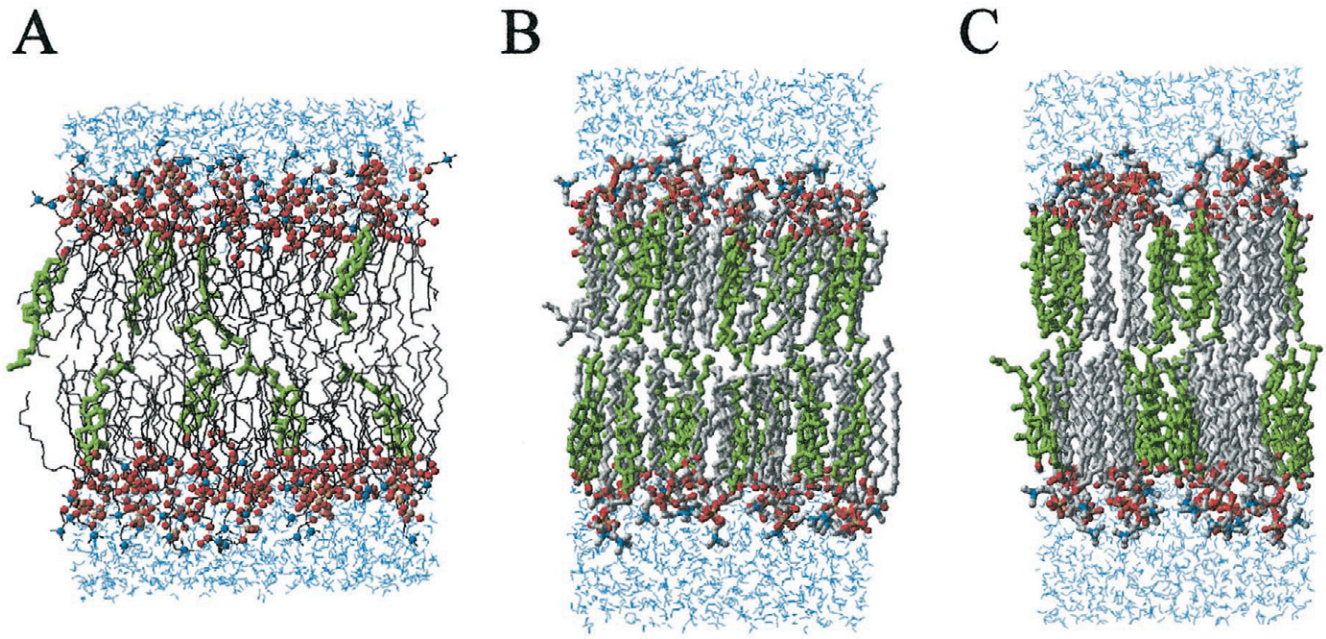


FIGURE 5 Side views of bilayers with 11 mol % cholesterol (*panel A*) and two bilayers with 50 mol % cholesterol: structure A (*panel B*) and structure B (*panel C*). Sterol molecules are shown as green sticks.

higher probability of finding the P-N vector pointing toward the bilayer interior than in the case of membranes with 50 mol % cholesterol. At the same time, the probability of finding smaller angles between the P-N vector and bilayer normal is comparable to the case when membranes contain 50 mol % cholesterol, and is higher than in the case of pure DPPC membrane. These two distinct populations are separated by a gap corresponding to the case when the P-N vector lies nearly parallel to the membrane surface. At 11 mol % cholesterol, we can distinguish two kinds of lipid molecules in bilayer: those in contact with cholesterol molecules and those further away from them. Since the average

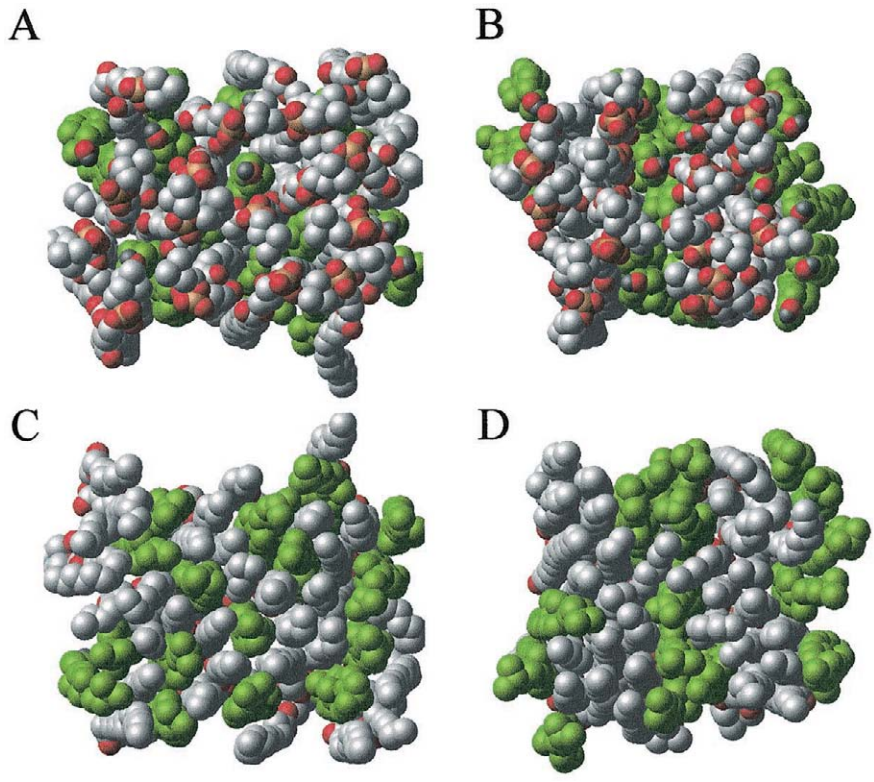


FIGURE 6 Views at the top and bottom of bilayer half in membranes with 50 mol % cholesterol: structure A (*panels A* and *C*, *top* and *bottom*, respectively) and structure B (*panels B* and *D*). Cholesterol and lipid molecules are shown using the CPK model. Carbon atoms of cholesterol are colored in green.

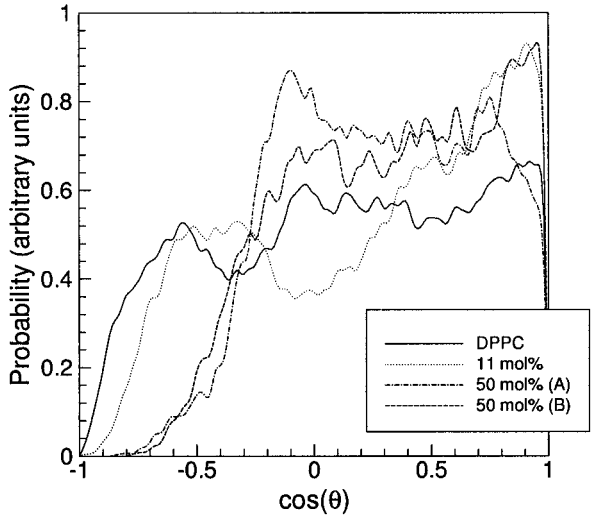


FIGURE 7 Distribution of the angle between P-N vector and bilayer normal in pure DPPC membrane (*solid line*) and in membranes with cholesterol: 11 mol % (*dotted line*), 50 mol % structure A (*dash-dotted line*), and structure B (*dashed line*). When cosine is positive, the P-N vector points into the water layer.

area per DPPC tails is lower than in pure DPPC membrane, lipid molecules located further away from sterols have a slightly lower average area per headgroup than in pure DPPC bilayer. In these molecules the P-N vector rises higher above the bilayer surface. Molecules in close contact with cholesterol have a slightly larger average area per headgroup. As a result, their headgroups are oriented parallel to the membrane surface and can even point toward the bilayer interior, since there are spaces at the level of lipid headgroups created when DPPC molecules were substituted by cholesterol molecules. This would account for the observed profile of the angle between the P-N vector and bilayer normal at low cholesterol content. In membranes with 50 mol % cholesterol we can have several possible mechanisms responsible for the headgroup behavior. In structure B, cholesterol and lipid molecules are packed in uniform stripes. Since the average area per lipid tails is decreasing compared to pure DPPC membranes, it is safe to assume that the average area per headgroup is also decreasing. As a result, the P-N vector is rising higher above the membrane surface, similar to the case of pure DPPC bilayer in gel phase. Another mechanism may be dominant in the case of structure A. It is known that in pure lipid bilayers, water molecules are forming bridges between adjacent lipid molecules (Pasenkiewicz-Gierula et al., 1997). It is possible that water bridging between lipid molecules becomes weaker as the average distance between DPPC molecules becomes larger in structure A at 50 mol % sterol compared to pure DPPC membrane. It is also possible that dipole-dipole interaction between DPPC headgroups decreases as the separation between the two lipid molecules becomes larger. The more energetically favorable conformation of the headgroup might be the one where the positively charged choline group is solvated by water molecules that form clathrate structures.

In Fig. 8 we show electron density profiles across the bilayer. We can see that differences between electron density profiles of pure DPPC bilayer and membrane with low cholesterol content are small. The addition of a small amount of cholesterol causes a small shift of peaks associated with the phosphate groups, while toward the bilayer center two profiles almost coincide. The addition of 50 mol % cholesterol results in further spreading of the electron density peaks. In addition, the shape of the profile changes slightly toward the bilayer center compared to the pure membranes: a flat region appears between the peaks and the minimum in the density profile in the middle of the membrane. Also, the electron density becomes slightly higher in the middle of the bilayer in membranes with 50 mol % cholesterol compared to pure DPPC membranes and membranes with 11 mol % cholesterol. The overall shape of the profile is similar to the one observed in neutron-scattering experiments on DMPC with 30 mol % cholesterol at $T = 50°C$ (Douliez et al., 1996). Experimentally observed hydrophobic thickness, which is defined as the distance between the peaks in the electron density profile, is increased by 4 Å in the DMPC bilayer with 30 mol % cholesterol (compared to the DMPC bilayer with 0 mol % sterol). The distance between two peaks computed in our simulations changes from 36 Å in pure DPPC bilayer to 37.2 Å at 11 mol % cholesterol. At 50 mol % cholesterol the peak-to-peak distances are 41.2 and 42.0 Å for structures A and B, respectively.

To characterize the changes in the bilayer interior in greater detail we calculated the average distances from the bilayer center to different atoms in DPPC molecules and compared them with the results obtained for the DPPC bilayer without cholesterol (see Table 2). The distance be-

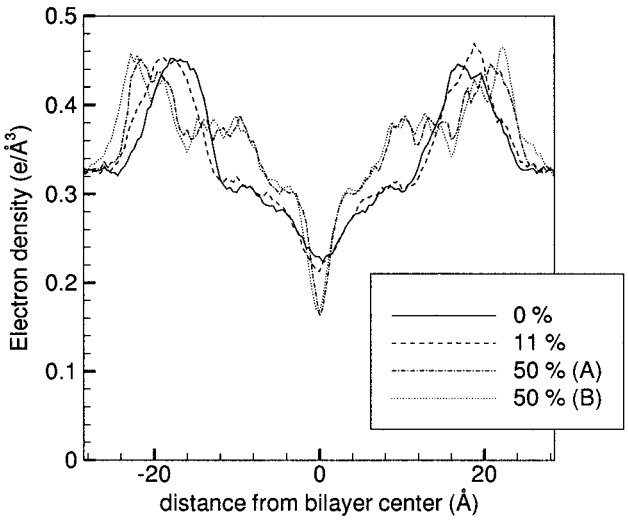


FIGURE 8 Electron density profiles in pure DPPC membrane (*solid line*) and in membranes with cholesterol: 11 mol % (*dashed line*), 50 mol % structure A (*dash-dotted line*), and structure B (*dotted line*).

tween phosphorus atoms increases with the increasing concentration of cholesterol (note that it is always slightly larger than the distance between the peaks in electron density profiles). In Fig. 9 we show distributions of phosphorus and nitrogen atoms, which provide details of the headgroup conformations, and the distributions of carbonyl oxygens in two ester groups. We also plotted distributions of water molecules and hydroxyl groups of cholesterol molecules. Distributions of atomic positions are broad in pure DPPC bilayers, while an increase in the cholesterol concentration results in the decrease of the width of the distributions of all lipid atoms. Regardless of the amount of cholesterol in lipid bilayer, the peak of the cholesterol's hydroxyl group distribution is located at the same distance from the bilayer center as the peak of the distribution of the carbonyl oxygens in DPPC. In all four systems considered in this work, pure DPPC bilayer in water and three systems with cholesterol added to DPPC, water molecules penetrated into the lipid membrane up to the carbonyl group. Similar observations have already been reported for bilayers in liquid crystal and gel phases by several other authors (Egberts et al., 1994; Berger et al., 1997; Tu et al., 1995, 1996). In membranes with 50 mol % cholesterol, water distribution decays in space slightly faster than the distribution of oxygen atoms in two carbonyl groups. This may indicate that water molecules penetrate up to the Sn-2 carbonyl group and in the lesser amount to the Sn-1 carbonyl group. The most pronounced changes were observed in the distributions of nitrogen atoms. Their distributions become sharper with increasing cholesterol concentrations and the peaks of the distribution shifted slightly away from the center of the bilayer, indicating that the choline group is rising higher above the plane of the membrane. This is in agreement with the measurements of the angle between the P-N vector and bilayer normal.

Inclusion of cholesterol molecules into the lipid bilayer reduces the area of DPPC molecules, which affects the structure of acyl chains. The ordering of hydrocarbon tails is usually characterized by the deuterium order parameter $S_{CD}$, which can be measured using the NMR technique. In computer simulations it can be calculated for each carbon in the lipid tail using the expression (Egberts and Berendsen, 1988):

$$S_{CD} = \frac{2}{3} S_{xx} + \frac{1}{3} S_{yy}, \qquad (1)$$

where $S_{ij} = \langle 1.5 \cos \theta_i \cos \theta_j - 0.5\delta_{ij} \rangle$ and $\theta_i$ is the angle between the $i$th molecular axis and the bilayer normal ($z$ axis). In Fig. 10 we compare $|S_{CD}|$ for different carbon atoms in the hydrocarbon chains, obtained for systems with different cholesterol concentrations, with the results for the pure DPPC bilayer. While the addition of 11 mol % cholesterol changes the order parameter only slightly, the addition of 50 mol % cholesterol increases values of $S_{CD}$ by almost a factor of 2. Experiments done on DMPC bilayers with 30 mol % cholesterol (Douliez et al., 1995; Sankaram

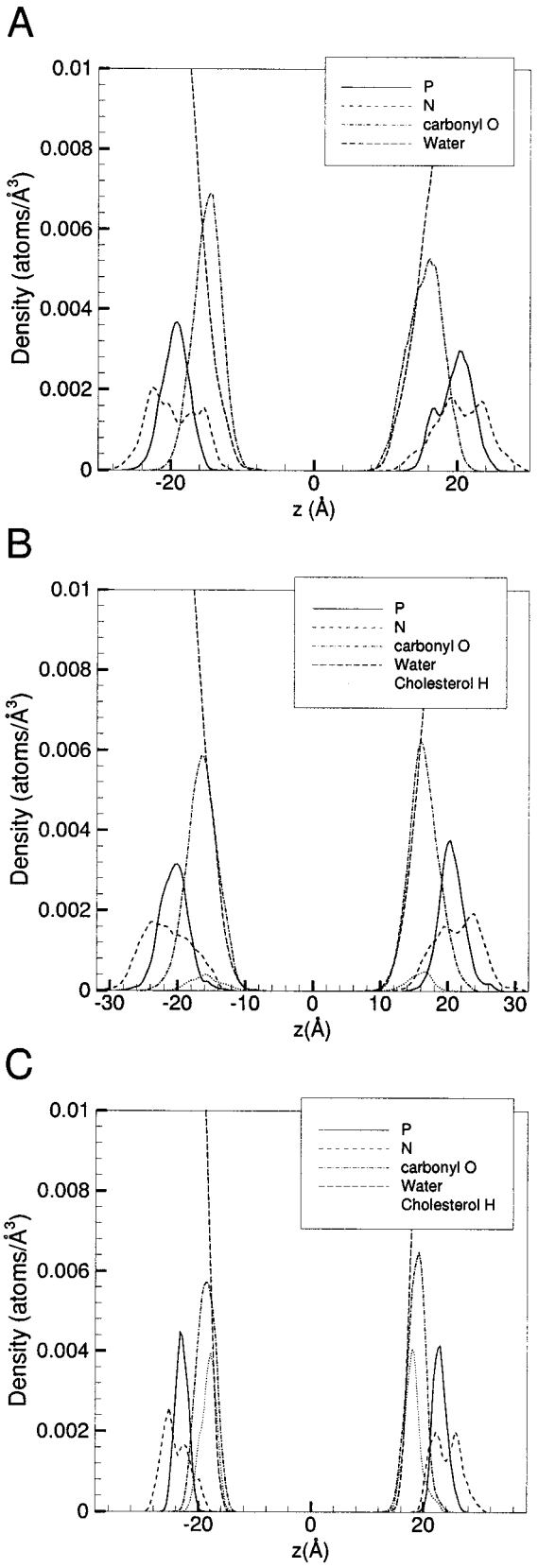


FIGURE 9 Distribution of atom positions along the bilayer normal in pure DPPC membrane (*panel A*), membrane with 11 mol % (*panel B*), and membrane with 50 mol % cholesterol in structure B (*panel C*).

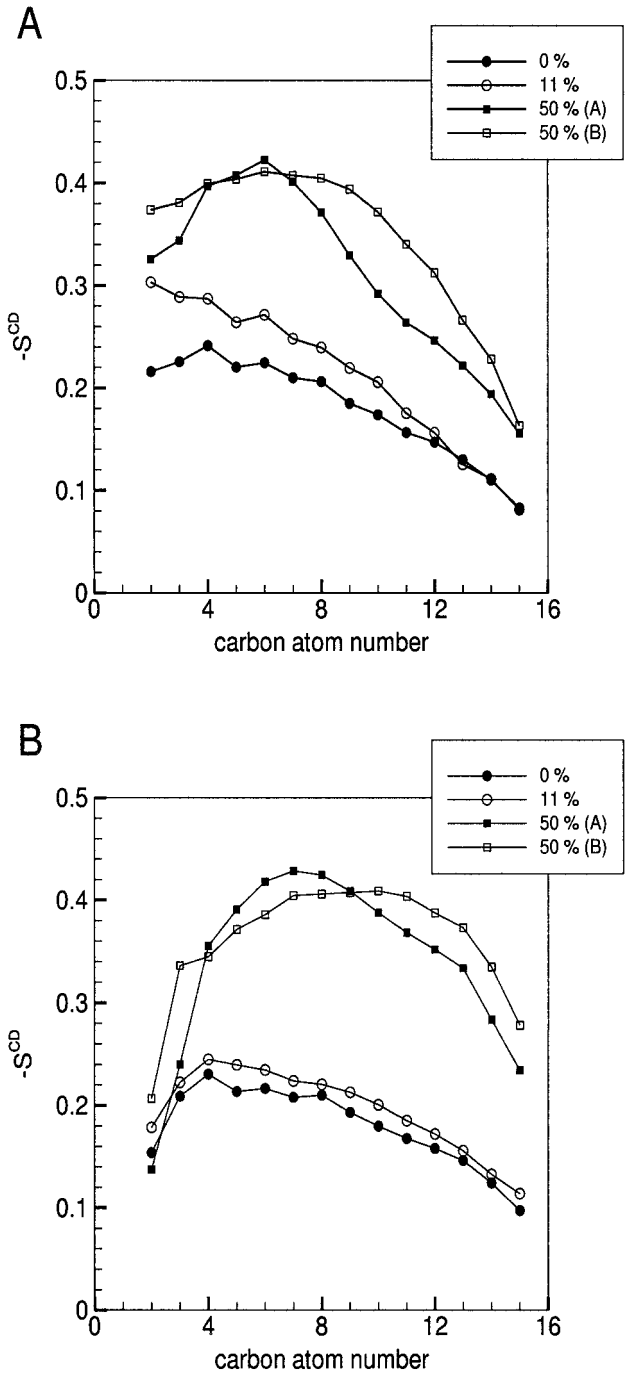


FIGURE 10 $S_{CD}$ order parameter as a function of carbon atom position for pure DPPC bilayer and DPPC bilayers with cholesterol in Sn-1 (*A*) and Sn-2 (*B*) tails.

and Thompson, 1990; Urbina et al., 1995) show a similar trend. In addition, the changes in the order parameter profiles are different for two chains and depend on the position of the carbon atoms. Increasing the concentration of cholesterol results in large changes for the order parameter in the middle of the hydrocarbon tails and smaller changes in the beginning and the end of the tails. Similar profiles were observed in experiments with DMPC at 30 mol % cholesterol (Urbina et al., 1995). Recent experiments on DMPC/cholesterol bilayers (Guerneve and Auger, 1995) indicate that the effect of cholesterol is mostly due to its interactions with the acyl chains, but it is not uniform along the nonpolar region of DMPC. NMR spectroscopic studies (Morrow et al., 1995) showed that cholesterol significantly increases the order parameter in the plateau region, but progressively less so toward the methyl ends of these chains. Similar behavior was also observed in the present simulations. Inclusion of cholesterol into lipid membrane has lesser effect on the order parameter of the second carbon atom in Sn-1 and Sn-2 chains. This might be due to the location of the cholesterol molecules inside the bilayer. The cholesterol hydroxyl group is located below the lipid's Sn-2 chain carbonyl groups, so that the first carbon atoms in acyl chains do not interact strongly with cholesterol molecules, especially in Sn-2 chains. In Fig. 11 we plotted the $S_{CD}$ order parameters in two chains (membrane with 50 mol % cholesterol, structure B) as a function of the distance between carbon atoms and the center of the bilayer, rather than the carbon atom number. We can see that profiles for two chains look very much alike, especially in the range marked by dashed lines, where lipid tails interact with the sterol's ring system. Such behavior is not observed in pure DPPC bilayers. This result indicates that changes in the ordering of hydrocarbon tails due to the inclusion of cholesterol depend on the distance from the bilayer center rather than the number of the carbon atom in the acyl chain. The differences in order parameter profiles for two different chains become more pronounced at distances where the lipid's hydrocarbon tails interact with cholesterol tails rather than with rigid cholesterol rings. We can clearly see that the plateau region of the $S_{CD}$ order parameters in both chains coincides with positions of the cholesterol rings (boundaries of cholesterol rings are shown in Fig. 11 as *dashed lines*).

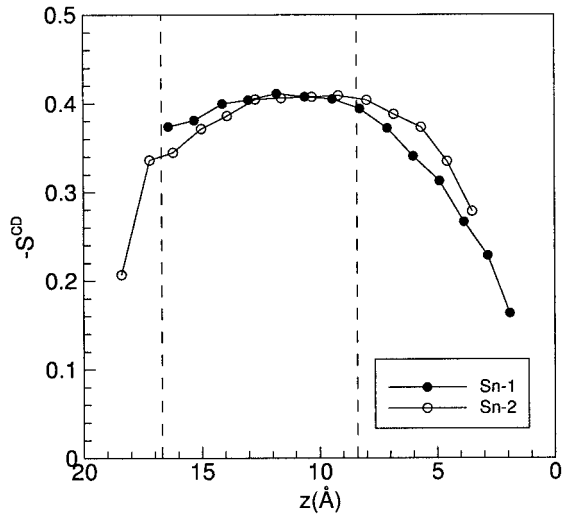


FIGURE 11 $S_{CD}$ order parameter as a function of the distance from bilayer center. Vertical dashed lines indicate positions of carbon atoms $C_3$ and $C_{17}$ in cholesterol, which mark the beginning and end of the sterol's ring system.

The changes in the chain ordering can be also characterized through the order parameter $\langle|S_{CD}|\rangle$, averaged over all carbon atoms in both chains. This value can be extracted from the first moment $M_1$ of the $^2$H-NMR spectrum. Ipsen et al. (1990) derived the NMR order parameter $2\langle|S_{CD}|\rangle$ from experimental data for the first momentum $M_1$ of magnetic resonance spectrum of DPPC bilayers containing cholesterol (Vist, 1984). Upon the addition of 10 mol % cholesterol the NMR order parameter increases from 0.31 (0 mol %) to 0.38. The same effect is seen in mean field calculations (Ipsen et al., 1990), where the NMR order parameter increases from 0.38 (0 mol %) cholesterol to 0.41 (10 mol %) and 0.78 (45 mol %) cholesterol. The corresponding values obtained from the present molecular dynamics simulations show the same trend: 0.34 (0 mol %), 0.38 (11 mol %), and 0.72 (50 mol %) cholesterol. A similar trend was also observed in experiments on DMPC/cholesterol model membranes. At 50 mol % cholesterol the molecular order parameter increased by a factor of ~2 compared to pure DMPC membrane (Rice et al., 1979; Kintanar et al., 1986).

More information about the ordering in hydrocarbon chains can be obtained from the $S^{CC}$ order parameter. It is given by the expression $S_n^{CC} = (1.5\cos^2(\phi_n) - 0.5)$, where $\phi_n$ is the angle between the bilayer normal and the bond connecting carbon atoms $C_{n-1}$ and $C_n$. For the Sn-1 chain the difference between the odd and even $S^{CC}$ order parameters, namely $S_3^{CC} < S_4^{CC}$, $S_5^{CC} < S_6^{CC}$ etc., constitutes a so-called "odd-even" effect (Douliez et al., 1995). The behavior of $S^{CC}$ is slightly different in Sn-2 chains than in Sn-1 chains. Experimental (Douliez et al., 1995) and simulation (Smondyrev and Berkowitz, 1999b) results indicate that at $T = 50$°C the $S^{CC}$ order parameter is almost constant in the beginning of the Sn-2 hydrocarbon chain in DPPC and decays monotonically toward the end of the tail. At higher temperatures or upon addition of cholesterol the odd-even effect is in the counter phase to the Sn-1 chain, i.e., for Sn-2 chains $S_3^{CC} > S_4^{CC}$ and $S_5^{CC} > S_6^{CC}$ (Douliez et al., 1995). The plots of $S^{CC}$ order parameter for three cholesterol containing bilayers are shown in Fig. 12. We can see that for 11 mol % and 50 mol % cholesterol (structure B) $S^{CC}$ profiles behave as predicted by the experiment (Douliez et al., 1995, 1996). Interestingly, at 50 mol % cholesterol (structure A) we found that the amplitude of the odd-even effect in Sn-2 chains was very small compared with two other simulations of cholesterol-containing membranes. In the work of Douliez et al. (1996) it was suggested that the amplitude of the odd-even effect depends on the orientation of the first bond, which was characterized through the $C_1$–$C_2$ order parameter. In our simulations of pure DPPC membrane the $C_1$–$C_2$ order parameter was found to be 0.49 for the Sn-1 chain and 0.18 for the Sn-2 chain. Experimentally observed values at $T = 50$°C was −0.15 for the Sn-2 chain in pure DPPC membrane. Addition of cholesterol caused the $C_1$–$C_2$ order parameter to increase in Sn-1 and decrease in Sn-2 chains. Our simulations of cholesterol containing bilayers showed a similar trend. The values of the $C_1$–$C_2$ order parameter in Sn-2 chains were 0.16 (11 mol %), 0.15 (50 mol %, structure A) and 0.04 (50 mol %, structure B). The values of the $C_1$–$C_2$ order parameter in the Sn-1 chain did not change compared to the values found for pure DPPC membrane: 0.50 (11 mol %), 0.46 (50 mol %, structure A), and 0.50 (50 mol %, structure B). As we can see, the absence of the pronounced odd-even effect in the simulation of membrane with 50 mol % cholesterol (structure A) cannot be explained simply on the basis of the $C_1$–$C_2$ order parameter. It was also suggested (Douliez et al., 1998) that the initial bend in Sn-2 chains may be responsible for the different behavior of $S^{CC}$ order parameters in Sn-1 and Sn-2 chains. To characterize this bend we calculated torsional angles corresponding to rotations around $C_1$–$C_2$ and $C_2$–$C_3$ bonds.

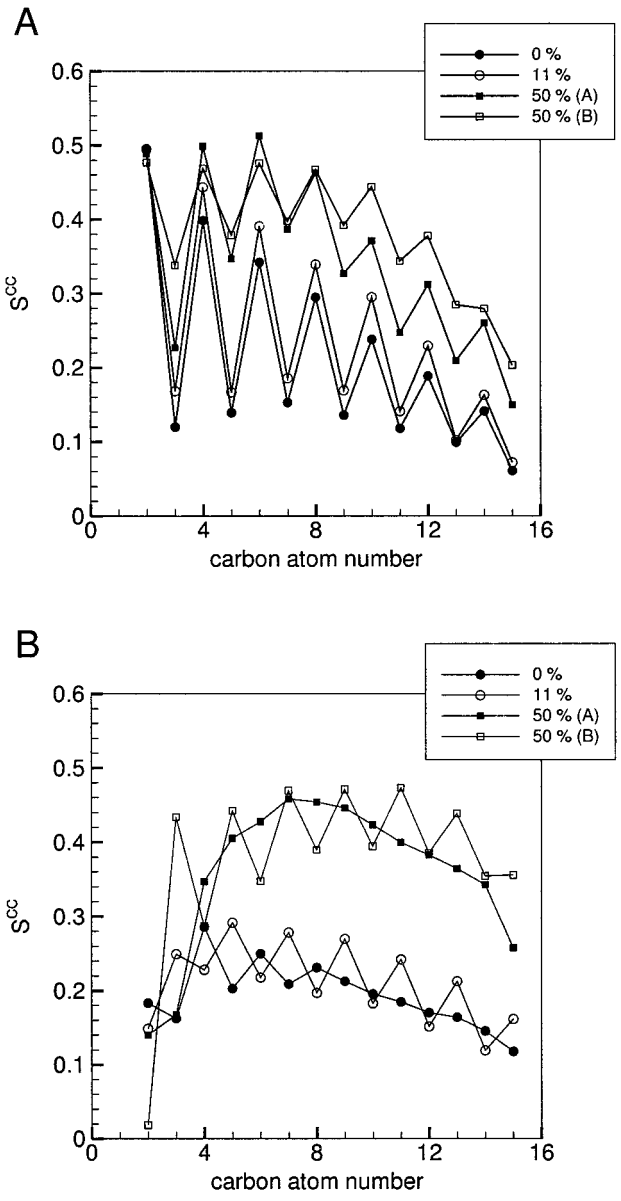


FIGURE 12 $S_{CC}$ order parameter profile in pure DPPC membrane and membranes with cholesterol in Sn-1 (*A*) and Sn-2 (*B*) tails.

According to the definition of Hauser et al. (1981) these dihedral angles are called $\beta_3$ and $\beta_4$ in the Sn-2 chain and $\gamma_3$, $\gamma_4$ in the Sn-1 chain. In Fig. 13 we plotted torsional angle $\beta_4$ vs. $\beta_3$ obtained in simulations of pure DPPC bilayers and in three simulations of mixed DPPC/cholesterol membranes. As we can see from this figure these maps are very similar in all three cases when membranes contain cholesterol molecules. This indicates that the initial bend in all three cases is very similar and that it may not be the only factor responsible for the appearance of the odd-even effect in Sn-2 chains. By comparing maps of torsional angles for membranes with cholesterol with the one in the case of pure DPPC bilayer, it is evident that inclusion of cholesterol results in suppression of some possible conformations of the first two dihedral angles. Instead of uniform distribution of points, as in the case of pure DPPC membrane, we see several localized domains with high point populations. It suggests that the inclusion of cholesterol restricts the motion of carbon atoms in the beginning of DPPC hydrocarbon tails. Our results show that in the cholesterol-containing membranes the odd-even effect is sensitive not only to the bend in the beginning of the chains, but also to the difference in the arrangements of cholesterol molecules in the membranes, as evident in the case of 50 mol % cholesterol (structure A).

The conformational properties of phospholipid chains can also be characterized by the average number of *gauche* defects. The total number of *gauche* defects per DPPC molecule is decreasing upon addition of cholesterol. The addition of 11 mol % cholesterol decreases the number of *gauche* defects only slightly: 6.7 per DPPC molecule, compared to 7.0 in pure DPPC membrane. Higher cholesterol concentrations caused a dramatic reduction in the number of *gauche* defects: 5.1 in structure A and 4.3 in structure B.

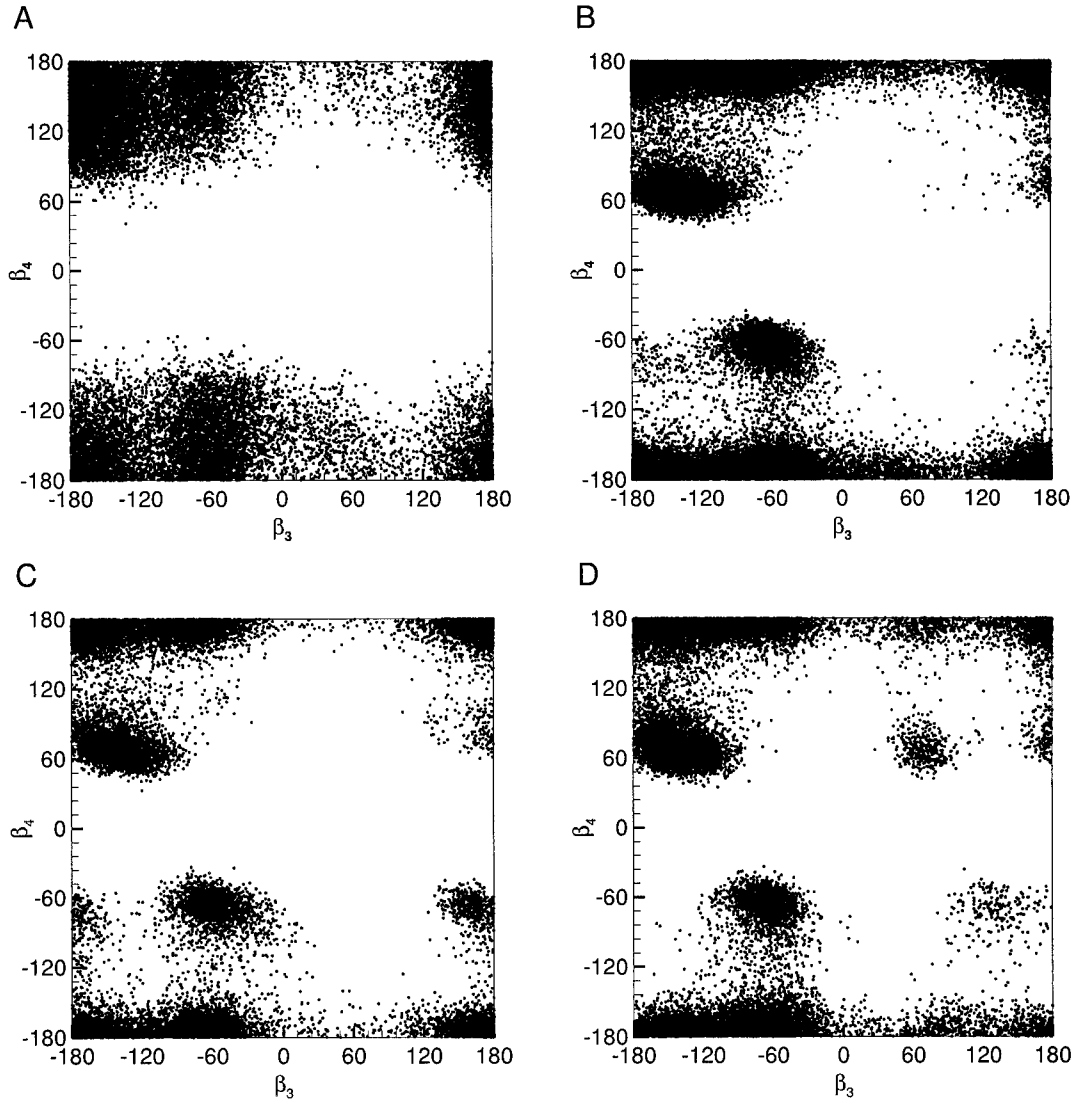


FIGURE 13 Maps of torsional angles in the beginnings of hydrocarbon chains. We plot $\beta_4$ vs. $\beta_3$ torsional angles in Sn-2 chain (notation after Hauser et al. (1981) for pure DPPC membrane (*A*), membrane with 11 mol % cholesterol (*B*), and two membranes with 50 mol % cholesterol: structure A (*C*) and structure B (*D*).

Again, the values obtained for the same (high) concentration of cholesterol depend strongly on the arrangement of cholesterol molecules in lipid membrane. Data obtained using infrared spectroscopy indicate that the number of *gauche* defects is decreasing from 3.9 per chain in DPPC to 1.2 in DPPC bilayer with 33% cholesterol (Mendelsohn et al., 1991). NMR results for DMPC + 30 mol % cholesterol at $T = 25°C$ (Douliez et al., 1995) indicate a factor of 3.7 decrease in the number of *gauche* defects.

An increase in the hydrocarbon chain order and decrease in the number of *gauche* defects is accompanied by the increase of the hydrocarbon chain lengths. The latter effect becomes more pronounced in membranes with 50 mol % cholesterol. In our recent simulations of pure DPPC bilayer we found that the lengths of two chains are similar: 13.6 and 13.4 Å for Sn-1 and Sn-2 chains, respectively. In bilayers with 11 mol % cholesterol, chain lengths did not change (compared to pure DPPC membrane): 13.6 and 13.2 Å for Sn-1 and Sn-2, respectively. In membranes with high cholesterol concentrations hydrocarbon chains become more extended. For structure A (50 mol % cholesterol) the lengths of the chains were 15.3 and 16.1 Å for Sn-1 and Sn-2 tails correspondingly, while in structure both these values were 16.8 Å.

Another important characteristic of lipid bilayers that is varied with the incorporation of cholesterol molecules in membranes is the dipole potential. It can be calculated from the expression:

$$\psi(z) - \psi(0) = -\int_0^z dz' \int_0^{z'} \rho(z'')dz'' \qquad (2)$$

where $\rho(z)$ is the local excess charge density. In Fig. 14 we show the total potentials for different concentrations of cholesterol. The addition of 11 mol % cholesterol had little effect on the magnitude of the total dipole potential. For bilayers with 50 mol % cholesterol we found a noticeable increase in the magnitude of the potential: from ~600 mV in pure DPPC and DPPC + 11 mol % cholesterol bilayers to ~900–1000 mV in bilayers with 50 mol % cholesterol. Measurements on egg PC monolayers (McIntosh et al., 1989) showed that the magnitude of the dipole potential is increasing with the addition of cholesterol. A similar trend was found in bilayers with keto-cholestanol (Voglino et al., 1998).

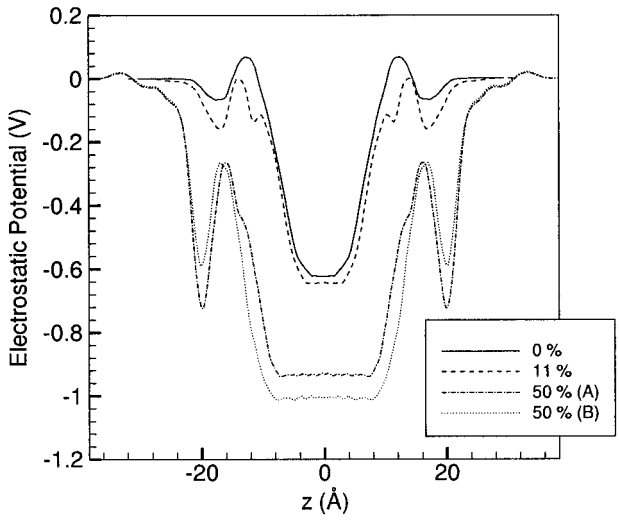


FIGURE 14 Dipole potential in pure DPPC membrane and three membranes with cholesterol.

To obtain more information about the organization of sterol-containing membranes we determined the location of cholesterol molecules inside the bilayer. First we calculated the tilt of cholesterol molecules by measuring the angle between vector-connecting cholesterol carbon atoms C3 and C17 (see Fig. 1) and the normal to the bilayer. At low cholesterol concentration this angle is 20 ± 3°, while at high concentration the tilt is decreasing to 11 ± 1° and 12.3 ± 1.3° in structures A and B, respectively. The values of the cholesterol tilt angles are close to the values found in recent simulations of DPPC membrane with 12.5% mol cholesterol (~14°) (Tu et al., 1998) and experiments on DMPC membranes with various amounts of cholesterol (~16–18° depending on the temperature and cholesterol concentration) (Oldfield et al., 1978). More recently, Marsan et al. (1999) showed that the absolute values of the cholesterol tilt depend on the models and assumptions used for their determination. Authors reported values of the molecular order parameter for DMPC membranes with 16 and 30 mol % cholesterol at 30°C, from which one can estimate the cholesterol tilt angles as ~15.7° and ~10.5° correspondingly. Also, cholesterol molecules become more tilted with the increase of temperature. Although it is hard to make a comparison between our results and the data from the experiment (Marsan et al., 1999) since the latter was performed on DMPC membrane, the observed trend is correct. Cholesterol molecules become more tilted when the thickness of membrane becomes smaller either as a result of the changes in cholesterol concentration or as a result of temperature variations. We should also point out that our definition of the cholesterol tilt is not unique. Nevertheless, it allows us to observe qualitative changes occurring in the membrane. We also determined positions of different atoms in cholesterol molecules relative to the bilayer center. In Table 3 we show the distances to H (hydrogen atom in hydroxyl group), C3, C17, and C26(27) atoms in cholesterol. We can see that on average, cholesterol molecules are located below the carbon atom G3 in DPPC molecules. In structure A (50 mol % cholesterol) the hydroxyl group of cholesterol is found ~0.5 Å closer to the DPPC headgroup than in structure B. At the same time the distance between phosphorus atoms and the middle of the bilayer is larger by ~1 Å in structure B compared to structure A. Positioning of cholesterol molecules along the bilayer normal is correlated to the overall tilt of sterols. In Fig. 15 we plot the distance between the cholesterol hydroxyl group and bilayer center as a function of the cholesterol molecule tilt angle. In bilayers with 50 mol % cholesterol the range of possible tilt

**TABLE 3 Average distances from bilayer center to atoms in cholesterol molecules, cholesterol tilt angle, the length of cholesterol projection on axis parallel to bilayer normal, and average lengths of DPPC hydrocarbon chains**

| | 11 mol % | 50 mol % (A) | 50 mol % (B) |
|---|---|---|---|
| Cholesterol | | | |
| Tilt | 20 ± 3 | 11 ± 1 | 12.3 ± 1.3 |
| HO | 15.5 ± 0.4 | 18.2 ± 0.2 | 18.4 ± 0.2 |
| C3 | 14.0 ± 0.3 | 16.6 ± 0.2 | 16.7 ± 0.2 |
| C17 | 6.0 ± 0.4 | 8.2 ± 0.2 | 8.4 ± 0.2 |
| C26(27) | 1.5 ± 0.4 | 1.8 ± 0.2 | 2.3 ± 0.2 |
| Cholesterol length | 14.0 ± 0.4 | 16.4 ± 0.2 | 16.1 ± 0.2 |
| DPPC | | | |
| Sn-1 chain length | 13.6 ± 0.4 | 15.3 ± 0.3 | 16.8 ± 0.2 |
| Sn-2 chain length | 13.2 ± 0.2 | 16.1 ± 0.2 | 16.8 ± 0.2 |

Note the values for the length of cholesterol's projection along the bilayer normal is very similar to the lengths of DPPC tails.

angles is relatively narrow, and the position of the cholesterol hydroxyl group relative to the bilayer center is correlated to the tilt angle. In bilayers with 11 mol % cholesterol the range of possible tilt angles is wider than in membranes with high sterol content. The location of the hydroxyl group is not strongly correlated with the tilt angle. The maximum and minimum tilt angles in all membranes containing cholesterol depend on the hydrophobic thickness of the lipid molecules. We suggest that the maximum tilt angle is limited due to the steric interactions with molecules in the same monolayer, while the minimum angle is defined so that the cholesterol molecule would not penetrate into the opposite half of the bilayer. The projection of the length of the cholesterol molecules on the normal to the bilayer, calculated as the distance between the hydroxyl group and methyl groups in the cholesterol tail, matches the length of the hydrocarbon tails (see Table 3). At low cholesterol concentrations (11 mol %), the lipid's hydrocarbon chains do not have high order and their lengths are comparable with the ones in pure DPPC membranes. In crystal structures the cholesterol molecule has a length of ~17 Å. To fit into the lipid bilayer, taking into the account that the cholesterol hydroxyl group is located slightly below the first carbon atom in DPPC chains, the cholesterol molecule has to tilt with respect to the bilayer normal. In addition, the appearance of the *gauche* defects in cholesterol tails can further reduce its length. At high cholesterol concentrations the DPPC acyl chains are highly ordered and their length becomes similar to the length of cholesterol molecules. Since cholesterol molecules are only slightly longer, they need to tilt by a small angle relative to the bilayer normal. It was argued that the mean hydrophobic length of cholesterol is equal to the one of the 17:0 PC molecule (McMullen et al., 1993). The DPPC (16:0 PC) molecule is slightly shorter, and this fact may explain the observed tilt of cholesterol molecules.

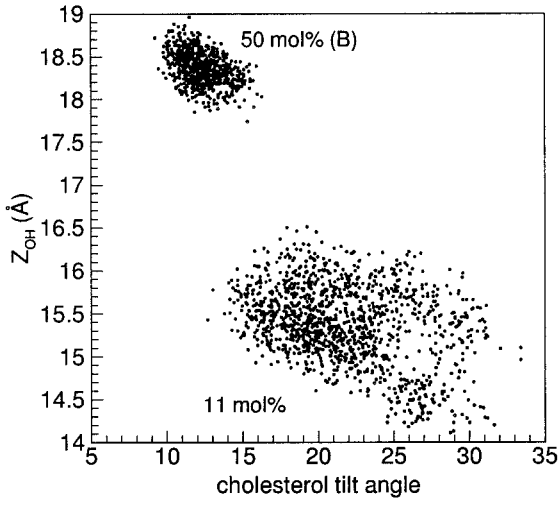


FIGURE 15 Position of cholesterol hydroxyl group relative to the bilayer center as a function of cholesterol tilt angle in membranes with 11 and 50 (structure B) mol % cholesterol. For bilayer with 50 mol % cholesterol (structure A) the picture (not shown for clarity) is similar to the one obtained for structure B. Its center is slightly shifted relative to the center of the distribution of points in structure B.

We also calculated the average number of hydrogen bonds formed among cholesterol, DPPC, and water molecules. We defined the hydrogen bond using the following criteria (Pasenkiewicz-Gierula et al., 1997): the distance between water or cholesterol oxygen and the DPPC oxygen is shorter than 3.25 Å and the angle between the vector linking DPPC oxygen with water (or cholesterol) oxygen and the H–O bond of the water (or cholesterol) is $<35°$, as proposed by Raghavan et al. (1992). In Table 4 we listed the average number of hydrogen bonds formed between DPPC oxygens and water molecules per DPPC molecule, and the average number of hydrogen bonds between DPPC oxygens and cholesterol per cholesterol molecule. We can see that the average number of hydrogen bonds with water molecules does not depend on the cholesterol concentration. Our numbers are very similar to those obtained in simulations of DMPC membrane (Pasenkiewicz-Gierula et al., 1997), except that we observe higher numbers of hydrogen bonds formed with carbonyl oxygens. This is consistent with the observations that water molecules penetrate into the lipid bilayer up to the carbonyl groups. We also found that the average number of hydrogen bonds formed with carbonyl oxygen of Sn-2 chain is approximately three times larger than the one with the carbonyl oxygen belonging to the Sn-1 chain. This result agrees with the data obtained using IR spectroscopy (Wong and Mantsch, 1988). It is also reasonable, since the Sn-1 carbonyl group is located closer to the bilayer center than the Sn-2 carbonyl group. On average, DPPC makes ~6.2 hydrogen bonds with water molecules regardless of cholesterol content. Some water molecules are simultaneously bonded to two different DPPC oxygens forming intermolecular or intramolecular water bridges. The average number of hydrogen bonds per DPPC molecule involved in formation of water bridges is ~2.2 in pure DPPC membrane and membrane with 11 mol % cholesterol. At 50 mol % cholesterol the number of water bridges is decreasing, as is evident by the average number of hydrogen

**TABLE 4 Average number of hydrogen bonds per DPPC or cholesterol oxygens, formed with water and cholesterol molecules as indicated**

| | Pure DPPC | 11 mol % | | 50 mol % (A) | | 50 mol % (B) | |
|---|---|---|---|---|---|---|---|
| | (water) | water | cholesterol | water | cholesterol | water | cholesterol |
| $O_{12}$ | 0.53 | 0.59 | 0 | 0.55 | 0.001 | 0.56 | 0 |
| $O_{11}$ | 0.22 | 0.22 | 0.10 | 0.26 | 0.12 | 0.33 | 0.005 |
| $O_{14}$ | 1.67 | 1.61 | 0 | 1.73 | 0.03 | 1.71 | 0.02 |
| $O_{13}$ | 1.70 | 1.66 | 0.003 | 1.63 | 0.0 | 1.72 | 0.005 |
| $O_{22}$ | 1.38 | 1.45 | 0.09 | 1.46 | 0.12 | 1.29 | 0.30 |
| $O_{32}$ | 0.54 | 0.54 | 0.13 | 0.52 | 0.03 | 0.67 | 0.07 |
| Total H-bonds | 6.04 | 6.07 | | 6.15 | | 6.31 | |
| Bonds in bridges | 2.23 | 2.24 | | 1.67 | | 1.64 | |
| $O_{CHOL}$ | | 0.72 | | 0.89 | | 0.97 | |

Also shown are the total number of hydrogen bonds with water molecules per DPPC and the number of hydrogen bonds involved in bridging between DPPC molecules.

bonds (~1.6 per DPPC molecule). In structure B, this 25% decrease can be attributed to the fact that on average, a DPPC molecule has three DPPC and one cholesterol molecule as nearest neighbors. In structure A the decrease in the number of water bridges may be due to the increase in the average distance between DPPC molecules.

Cholesterol forms hydrogen bonds differently depending on its concentration and arrangement in the lipid bilayer. The most probable sites to form hydrogen bonds with cholesterol's hydroxyl group are carbonyl oxygens and ester P-oxygen $O_{11}$, which is the closest to the bilayer center among all four phosphorus oxygens. At low concentrations cholesterol can form hydrogen bonds with any of these three sites with almost equal probabilities (see Table 4). At high concentrations (structure B) the probabilities of forming hydrogen bonds with ester P-oxygen and carbonyl oxygen on the Sn-1 chain become lower and most of the hydrogen bonds are formed with Sn-2 chain carbonyl oxygen. In structure A the situation is slightly different. While the probability of forming a hydrogen bond with Sn-1 carbonyl oxygen remains relatively low, the probabilities of forming hydrogen bonds with Sn-2 carbonyl oxygen or ester P-oxygen are almost the same. Cholesterol can also form hydrogen bonds with water molecules. The average number of hydrogen bonds is comparable for two membranes with 50 mol %: 0.89 (structure A) and 0.97 (structure B), and is slightly lower for membrane with 11 mol % cholesterol (0.72). In membranes with 11 mol % sterol, cholesterol molecules can move deeper toward the middle of the bilayer so that their hydroxyl group becomes less exposed to water. At 50 mol % cholesterol such motions are restricted (as seen in Fig. 15), and as a result the number of hydrogen bonds formed between cholesterol and water molecules is slightly higher. This can be shown by calculating the average number of hydrogen bonds between cholesterol and water as a function of distance between the hydroxyl group of cholesterol and the bilayer center. In membranes with 11 mol % cholesterol the probability of forming the hydrogen bond becomes slightly lower when the cholesterol molecule is located deeper inside the bilayer. This is clearly due to the fact that water molecules can penetrate inside the bilayer only up to a carbonyl group. In membranes with 50 mol % cholesterol this probability is almost independent of distance from the bilayer center. This is due to the fact that at high sterol concentrations cholesterol molecules cannot be placed deep inside the membrane and their hydroxyl groups are exposed to water.

## CONCLUSIONS

We performed three simulations of DPPC membranes with cholesterol: one with a low (11 mol %) and two with high (50 mol %) concentrations of cholesterol. We studied the properties of the bilayers with 50 mol % cholesterol for two different initial packing structures. In one simulation cholesterol molecules were distributed regularly in membrane, while in the second simulation lipid (cholesterol) molecules were placed in lipid- (cholesterol)-rich striped domains. The results of these simulations were compared with the data obtained from our recent simulation of pure DPPC membrane. Each simulation of bilayer with cholesterol was run for 2.0 ns. Our data indicate that rather long equilibration times are required to allow the system to reach equilibrium. The usage of the constant pressure algorithm allowed us to study the changes in the membrane geometry due to the inclusion of cholesterol. We found that the addition of 50 mol % cholesterol to lipid membrane results in a large reduction of the membrane area. It should be noted that although the average area occupied by hydrocarbon tails is reduced, the area per headgroup increases on the average since cholesterol molecules are located below the DPPC carbonyl groups. In structure A the membrane area continued to drift slowly even during the last 1 ns of simulation rather than converging to a constant value, as in structure B. The area of the membrane with 11 mol % cholesterol also decreased, but much less than in the case of large cholesterol concentrations. Compression of lipid bilayers was accompanied by the increasing order in hydrocarbon tails, which was most pronounced in bilayers with 50 mol % cholesterol. We found that in membranes with 50 mol % cholesterol when molecules were arranged in striped do-

mains their order was higher than when they were distributed in a regular fashion. In Sn-2 chains the amplitude of the odd-even effect increased with the addition of cholesterol (as seen in the experiments) except for the 50 mol % cholesterol structure A membrane. We observed several differences in our simulations in the properties of membranes with 50 mol % cholesterol, such as drift in membrane area, lower order in hydrocarbon chains, and lower amplitude of the odd-even effect in structure A compared to structure B. These results may suggest that at high cholesterol concentrations, structures with cholesterol-rich domains are more favorable, while membranes with uniform cholesterol distributions are in a metastable state. Our simulation times were not sufficiently long to test this hypothesis directly. The lipid membrane hydrophobic thickness varied in accordance with the cholesterol concentration and its distribution. The locations of cholesterol molecules also varied accordingly by adjusting the tilt angle to accommodate in the membrane. At low cholesterol content, tails of DPPC molecules are disordered and hydrophobic thickness is comparable to the one in the pure DPPC bilayer. Cholesterol molecules exhibit a large tilt, so that sterol and DPPC hydrophobic thicknesses match. At 50 mol % sterol DPPC tails are more ordered, their length is larger, and as a result cholesterol tilt is decreasing. Cholesterol motion along the bilayer normal becomes more restricted with the increase in sterol concentration. We also determined the average number and most probable atoms with which cholesterol molecules formed hydrogen bonds. We found that cholesterol can form hydrogen bonds with oxygens in DPPC carbonyl groups and one of the oxygens in the DPPC phosphate group. Relative probabilities varied with cholesterol concentrations and its distribution. Water molecules can also form hydrogen bonds with cholesterol. At high cholesterol content the probability of finding a hydrogen bond between water and cholesterol did not depend on the position of the cholesterol molecule relative to the bilayer center. At low cholesterol content we found a slight drop in the hydrogen bonding probability, as the cholesterol molecules were located deeper inside the bilayer. We found that the average value of the angle between vector-connecting phosphorus and nitrogen atoms in DPPC and the surface of membrane is increasing from 9° in pure DPPC membrane to ~17° in membranes with cholesterol. The latter value varies with cholesterol concentration and its arrangement in membranes. It is possible that tilting of the P-N vector toward the bilayer normal rather than to the membrane surface may be related to the weakening of water bridges between lipid molecules. Our results indicate that the average number of hydrogen bonds with water molecules per lipid does not depend on the headgroup orientation.

Calculations were performed on Cray-T3Es at San Diego Supercomputer Center and Texas Advanced Computing Center. Computational support from NPACI is gratefully acknowledged.

This work was supported by National Science Foundation Grant MCB9604585.

## REFERENCES

Almeida, P. F. F., W. L. C. Vaz, and T. E. Thompson. 1992. Lateral diffusion in the liquid phases of dimyristoylphosphatidylcholine/cholesterol lipid bilayers: a free volume analysis. *Biochemistry.* 31: 6739–6747.

Berger, O., O. Edholm, and F. Jähnig. 1997. Molecular dynamics simulations of a fluid bilayer of dipalmitoylphosphatidylcholine at full hydration, constant pressure, and constant temperature. *Biophys. J.* 72: 2002–2013.

Chong, P. L. G. 1994. Evidence for regular distribution of sterols in liquid crystalline phosphatidylcholine bilayers. *Proc. Natl. Acad. Sci. USA.* 91:10069–10073.

Craven, B. M., and G. T. DeTitta. 1976. Cholesterol myristate: structures of the crystalline solid and mesophases. *J. Chem. Soc. Perkin Trans. 2.* 814–822.

Douliez, J. P., A. Ferrarini, and E. J. Dufourc. 1998. On the relationship between C–C and C–D order parameters and its use for studying the conformation of lipid acyl chains in biomembranes. *J. Chem. Phys.* 109:2513–2518.

Douliez, J. P., A. Léonard, and E. J. Dufourc. 1995. Restatement of order parameter in biomembranes: calculation of C–C bond order parameters from C–D quadrupolar splittings. *Biophys. J.* 68:1727–1739.

Douliez, J. P., A. Léonard, and E. J. Dufourc. 1996. Conformational order of DMPC sn-1 versus sn-2 chains and membrane thickness: an approach to molecular protrusion by solid state $^2$H-NMR and neutron diffraction. *J. Phys. Chem.* 100:18450–18457.

Egberts, E., and H. J. C. Berendsen. 1988. Molecular-dynamics simulation of a smectic liquid crystal with atomic detail. *J. Chem. Phys.* 89: 3718–3732.

Egberts, E., S. J. Marrink, and H. J. C. Berendsen. 1994. Molecular dynamics simulation of phospholipid membrane. *Eur. Biophys. J.* 22: 423–436.

Engelman, D. M., and J. E. Rothman. 1972. The planar organization of lecithin-cholesterol bilayers. *J. Biol. Chem.* 247:3694–3697.

Frisch, M. J., G. W. Trucks, H. B. Schlegel, G. E. Scuseria, M. A. Robb, J. R. Cheeseman, V. G. Zakrzewski, J. A. Montgomery, R. E. Stratmann, J. C. Burant, S. Dapprich, J. M. Millam, A. D. Daniels, K. N. Kudin, M. C. Strain, O. Farkas, J. Tomasi, V. Barone, M. Cossi, R. Cammi, B. Mennucci, C. Pomelli, C. Adamo, S. Clifford, J. Ochterski, G. A. Petersson, P. Y. Ayala, Q. Cui, K. Morokuma, D. K. Malick, A. D. Rabuck, K. Raghavachari, J. B. Foresman, J. Cioslowski, J. V. Ortiz, B. B. Stefanov, G. Liu, A. Liashenko, P. Piskorz, I. Komaromi, R. Gomperts, R. L. Martin, D. J. Fox, T. Keith, M. A. Al-Laham, C. Y. Peng, A. Nanayakkara, C. Gonzalez, M. Challacombe, P. M. W. Gill, B. G. Johnson, W. Chen, M. W. Wong, J. L. Andres, M. Head-Gordon, E. S. Replogle, and J. A. Pople. 1998. Gaussian 98. Gaussian, Inc., Pittsburgh, PA.

Gabdouline, R. R., G. Vanderkooi, and C. Zheng. 1996. Comparison of structures of dimyrstoylphosphatidylcholine in the presence and absence of cholesterol by molecular dynamics simulation. *J. Phys. Chem.* 96: 15942–15946.

Guerneve, C. L., and M. Auger. 1995. New approach to study fast and slow motions in lipid bilayers: application to dimyrstoylphosphatidylcholine-cholesterol interactions. *Biophys. J.* 68:1952–1959.

Hauser, H., I. Pasher, R. H. Pearson, and S. Sundell. 1981. Preferred conformation and molecular packing of phosphatidylethanolamine and phosphatidylcholine. *Biochim. Biophys. Acta.* 650:21–51.

Hyslop, P. A., B. Morel, and R. D. Sauerheber. 1990. Organization and interaction of cholesterol and phosphatidylcholine in model bilayer membranes. *Biochemistry.* 29:1025–1038.

Ipsen, J. H., O. G. Mouritsen, and M. Bloom. 1990. Relationship between lipid membrane area, hydrophobic thickness, and acyl-chain orientational order. *Biophys. J.* 57:405–412.

Jorgensen, W. L., J. Chandrasekhar, J. D. Madura, R. W. Impey, and M. L. Klein. 1983. Comparison of simple potential functions for simulating liquid water. *J. Chem. Phys.* 79:926–935.

Kintanar, A., A. C. Kunwar, and E. Oldfield. 1986. Deuterium NMR spectroscopy study of the fluorescent probe DPH in model membrane systems. *Biochemistry.* 25:6517–6524.

Marsan, M. P., I. Muller, C. Ramos, F. Rodriguez, E. J. Dufourc, J. Czaplicki, and A. Milon. 1999. Cholesterol orientation and dynamics in dimyristoylphosphatidylcholine bilayers: a solid state deuterium NMR analysis. *Biophys. J.* 76:351–359.

McIntosh, T. J., A. D. Magid, and S. A. Simon. 1989. Cholesterol modifies the short-range repulsive interactions between phosphatidylcholine membranes. *Biochemistry.* 28:17–25.

McMullen, T. P. W., R. N. A. H. Lewis, and R. N. McElhaney. 1993. Differential scanning calorimetric study of the effect of cholesterol on the thermotropic phase behavior of a homologous series of linear saturated phosphatidylcholines. *Biochemistry.* 32:516–522.

McMullen, T. P. W., and R. N. McElhaney. 1996. Physical studies of cholesterol-phospholipid interactions. *Curr. Opin. Colloid Interface Sci.* 1:83–90.

Mendelsohn, R., M. A. Davies, H. F. Chuster, Z. Xu, and R. Bittman. 1991. $CD_2$ rocking modes as quantitative infrared probes of one-, two-, and three-bond conformational disorder in dipalmitoylphosphatidylcholine and dipalmitoylphosphatidylcholine/cholesterol mixtures. *Biochemistry.* 30:8558–8563.

Morrow, M. R., D. Singh, D. Lu, and C. W. M. Grant. 1995. Glycosphingolipid fatty acid arrangement in phospholipid bilayers: cholesterol effects. *Biophys. J.* 68:179–186.

Oldfield, E., M. Meadows, D. Rice, and R. Jacobs. 1978. Spectroscopic studies of specifically deuterium labeled membrane systems. Nuclear magnetic resonance investigation of the effects of cholesterol in model systems. *Biochemistry.* 17:2727–2740.

Pasenkiewicz-Gierula, M., Y. Takaoka, H. Miyagawa, K. Kitamura, and A. Kusumi. 1997. Hydrogen bonding of water to phosphatidylcholine in the membrane as studied by a molecular dynamics simulation: location, geometry, and lipid-lipid bridging via hydrogen-bonded water. *J. Phys. Chem.* 101:3677–3691.

Pearson, R. H., and I. Pascher. 1979. The molecular structure of lecithin dihydrate. *Nature.* 281:499–501.

Raghavan, K., M. R. Reddy, and M. L. Berkowitz. 1992. A molecular-dynamics study of the structure and dynamics of water between dilaurophosphatidylethanolamine bilayers. *Langmuir.* 8:233–240.

Rice, D. M., M. D. Meadows, A. O. Schieman, F. M. Goni, J. C. Gomez-Fernandez, M. A. Moscarello, D. Chapman, and E. Oldfield. 1979. Protein-lipid interactions. A nuclear magnetic resonance study of sarcoplasmic reticulum $Ca^{2+}$, $Mg^{2+}$-ATPase, liophilin, and proteolipid apoprotein-lecithin systems and a comparison with the effects of cholesterol. *Biochemistry.* 18:5893–5903.

Robinson, A. J., W. G. Richards, P. J. Thomas, and M. M. Hann. 1995. Behavior of cholesterol and its effect on headgroup and chain conformations in lipid bilayers: a molecular dynamics study. *Biophys. J.* 68:164–170.

Sankaram, M. B., and T. E. Thompson. 1990. Modulation of phospholipid acyl chain order by cholesterol. A solid-state $^2H$ nuclear magnetic resonance study. *Biochemistry.* 29:10676–10684.

Shieh, H. S., L. G. Hoard, and C. E. Nordman. 1981. The structure of cholesterol. *Acta Crystallogr. B.* 37:1538–1543.

Smith, W., and T. R. Forester. 1996. DL_POLY is a package of molecular simulation routines written by W. Smith and T. R. Forester, copyright The Council for the Central Laboratory of the Research Councils, Daresbury Laboratory at Daresbury, Nr. Warrington.

Smondyrev, A. M., and M. L. Berkowitz. 1999a. United atom AMBER force field for phospholipid membranes. Constant pressure molecular dynamics simulation of DPPC/water system. *J. Comput. Chem.* 20: 531–545.

Smondyrev, A. M., and M. L. Berkowitz. 1999b. Molecular dynamics study of Sn-1 and Sn-2 chain conformations in DPPC membranes. *J. Chem. Phys.* 110:3981–3985.

Smondyrev, A. M., and M. L. Berkowitz. 1999c. Molecular dynamics simulation of DPPC bilayer in DMSO. *Biophys. J.* 76:2472–2478.

Tu, K., M. L. Klein, and D. J. Tobias. 1998. Constant-pressure molecular dynamics investigation of cholesterol effects in a dipalmitoylphosphatidylcholine bilayer. *Biophys. J.* 75:2147–2156.

Tu, K., D. J. Tobias, and M. L. Klein. 1995. Constant pressure and temperature molecular dynamics simulations of a fully hydrated liquid crystal phase dipalmitoylphosphatidylcholine bilayer. *Biophys. J.* 69: 2558–2562.

Tu, K., D. J. Tobias, and M. L. Klein. 1996. Molecular dynamics investigation of the structure of a fully hydrated gel-phase dipalmitoylphosphatidylcholine bilayer. *Biophys. J.* 70:595–608.

Urbina, J. A., S. Pekerar, H. Le, J. Patterson, B. Montez, and E. Oldfield. 1995. Molecular order and dynamics of phosphatidylcholine bilayer membranes in the presence of cholesterol, ergosterol and lanosterol: a comparative study using $^2H$-, $^{13}C$-, and $^{31}P$-NMR spectroscopy. *Biochim. Biophys. Acta.* 1238:163–176.

Vanderkooi, G. 1991. Multibilayer structure of dimyristoylphosphatidylcholine dehydrate as determined by energy minimization. *Biochemistry.* 30:10760–10768.

Vanderkooi, G. 1994. Computation of mixed phosphatidylcholine-cholesterol bilayer structures by energy minimization. *Biophys. J.* 66: 1457–1468.

Vist, M. R. 1984. Partial phase behavior of perdeuterated dipalmitoylphosphatidylcholine-cholesterol model membranes. M.Sc. Thesis, University of Guelph, Ontario, Canada. 103.

Vist, M. R., and J. H. Davis. 1990. Phase-equilibria of cholesterol dipalmitoylphosphatidylcholine mixtures: H-2 nuclear magnetic-resonance and differential scanning calorimetry. *Biochemistry.* 29:451–464.

Voglino, L., T. J. McIntosh, and S. A. Simon. 1998. Modulation of the binding of signal peptides to lipid bilayers by dipoles near the hydrocarbon-water interface. *Biochemistry.* 37:12241–12252.

Weiner, S. J., P. A. Kollman, D. A. Case, U. C. Singh, C. Ghio, G. Alagonax, S. Profeta, and P. Weiner. 1984. A new force field for molecular mechanics simulation of nucleic acids and proteins. *J. Am. Chem. Soc.* 106:765–784.

Wong, P. T. T., and H. H. Mantsch. 1988. High-pressure infrared spectroscopic evidence of water binding sites in 1,2-diacyl phospholipids. *Chem. Phys. Lipids.* 46:213–224.

Zuckermann, M. J., J. H. Ipsen, and O. G. Mouritsen. 1993. Cholesterol and Membrane Models. L. X. Finegold, editor. CRC Press Inc., Boca Raton, Florida.